Inhalation Delivery of a Novel Diindolylmethane Derivative for the Treatment of Lung Cancer

Nkechi Ichite[1], Mahavir Chougule[2], Apurva R. Patel[1], Tanise Jackson[1], Stephen Safe[3,4], and Mandip Singh[1]

Abstract

The purpose of this study was to determine the anticancer efficacy of 1,1-bis (3′-indolyl)-1-(p-biphenyl) methane (DIM-C-pPhC$_6$H$_5$) by inhalation delivery alone and in combination with i.v. docetaxel in a murine model for lung cancer. An aqueous DIM-C-pPhC$_6$H$_5$ formulation was characterized for its aerodynamic properties. Tumor-bearing athymic nude mice were exposed to nebulized DIM-C-pPhC$_6$H$_5$, docetaxel, or combination (DIM-C-pPhC$_6$H$_5$ plus docetaxel) using a nose-only exposure technique. The aerodynamic properties included mass median aerodynamic diameter of 1.8 ± 0.3 μm and geometric SD of 2.31 ± 0.02. Lung weight reduction in mice treated with the drug combination was 64% compared with 40% and 47% in mice treated with DIM-C-pPhC$_6$H$_5$ aerosol and docetaxel alone, respectively. Combination treatment decreased expression of Akt, cyclin D1, survivin, Mcl-1, NF-κB, IκBα, phospho-IκBα, and vascular endothelial growth factor (VEGF) and increased expression of c-Jun NH$_2$-terminal kinase 2 and Bad compared with tumors collected from single-agent treatment and control groups. DNA fragmentation was also enhanced in mice treated with the drug combination compared with docetaxel or DIM-C-pPhC$_6$H$_5$ alone. Combination treatment decreased expressions of VEGF and CD31 compared with single-agent treated and control groups. These results suggest that DIM-C-pPhC$_6$H$_5$ aerosol enhanced the anticancer activity of docetaxel in a lung cancer model by activating multiple signaling pathways. The study provides evidence that DIM-C-pPhC$_6$H$_5$ can be used alone or in combination with other drugs for the treatment of lung cancer using the inhalation delivery approach. *Mol Cancer Ther; 9(11); 3003–14. ©2010 AACR.*

Introduction

Lung cancer is one of the leading causes of cancer deaths (9% of all cancer deaths) in the United States, and non–small cell lung cancer (NSCLC) accounts for 85% of all lung cancers (1). The lung is a common site of primary malignancy and for metastasis from other primary locations such as colon, breast, prostate, and other tumors. Response and remission in NSCLC patients remain relatively low despite advances in lung cancer treatment (1). Systemic or oral drug delivery is rarely successful because only a limited amount of the chemotherapeutic drug targets lung tumor sites even when administered at a high dose. Most chemotherapeutic drugs also act on normal cells inhibiting their growth, which results in toxic adverse effects. A poor clinical outcome in lung cancer treatment has been partly attributed to the inability to achieve therapeutic concentrations of drugs at the tumor site (2). Regional drug delivery has therefore generated interest among scientists as a strategy to achieve better efficacy for the treatment of lung cancer.

Localized delivery of aerosolized drugs to the lungs offers several advantages over systemic delivery including delivery of high concentration of the compounds at the target tissue, avoiding first-pass effect, improving efficacy, requiring lower drug dosing, and minimizing systemic side effects (3). Drug absorption is enhanced by the vast surface area of the lungs and relatively low proteolytic enzymatic activity in the lungs (4).

The potential of inhalation drug delivery for lung cancer treatment has been shown by several researchers in preclinical and clinical studies (5–10). For example, treatment of nude mice with liposomal 9-nitrocamptothecin aerosol for 8 or 10 weeks starting from week 9 after implantation of osteosarcoma tumors resulted in a highly significant decrease in the number of animals with disease, the total number of tumor foci in the lungs, and the size of the individual tumor nodules (7). One of the initial clinical studies evaluated the inhalation delivery of 5-fluorouracil by nebulization and reported beneficial effects in NSCLC patients (11). In recent years, phase I clinical studies using aerosolized 9-nitrocamptothecin (12), doxorubicin (13), and cisplatin (14) have been conducted in patients with primary or metastasized lung cancer who

Authors' Affiliations: [1]College of Pharmacy and Pharmaceutical Sciences, Florida A&M University, Tallahassee, Florida; [2]Department of Pharmaceutical Sciences, College of Pharmacy, University of Hawaii, Hilo, Hawaii; and [3]Institute of Biosciences and Technology; [4]Texas A&M Health Sciences Center, Houston, Texas

Note: N. Ichite and M. Chougule contributed equally to this work.

Corresponding Author: Mandip Singh, College of Pharmacy and Pharmaceutical Sciences, Florida A&M University, Tallahassee, FL 32307. Phone: 850-561-2790; Fax: 850-599-3813. E-mail: mandip.sachdeva@gmail.com

*American Association for **Cancer Research***

failed previous conventional treatments. Overall, aerosolized chemotherapy was found to be feasible and safe with obvious lower adverse side effects relative to systemic delivery.

Peroxisome proliferator-activated receptor γ (PPARγ) has been evaluated as a therapeutic target for the treatment of various cancer types including lung cancer (15–17). The use of PPARγ agonists in combination with taxane exhibited synergistic antitumor effects in breast cancer (18) and additive antitumor effects in thyroid carcinoma (19) cancer models. 1,1-Bis (3′-indolyl)-1-(*p*-biphenyl) methane (DIM-C-pPhC$_6$H$_5$; Fig. 1) is a PPARγ agonist that inhibits growth of colon (20, 21), bladder (22), prostate (23), and breast (24, 25) cancer cells and tumors.

These findings suggest that PPARγ agonists may be used as chemopreventive agents and/or as an adjunct in cancer chemotherapy. Docetaxel has been approved for the treatment of NSCLC patients and exhibits its cytotoxic effects due to decreased proliferation and induction of apoptosis through stabilization of microtubules. Several researchers have studied the combination of docetaxel and other agents for the treatment of lung cancer (26–30) and reported enhanced anticancer effects. Thus, like C-substituted diindolylmethane (DIM), taxanes have cytotoxic properties but act through different biological mechanisms (28, 30, 31). Our previous studies showed that DIM-C-pPhC$_6$H$_5$ in combination with docetaxel exhibits synergistic activity *in vitro* against NSCLC (32). However, the inhalation delivery of DIM-C-pPhC$_6$H$_5$ alone and in combination with standard chemotherapeutic agents for the treatment of lung cancer has not been determined.

Therefore, the purpose of this study was to examine the feasibility of aerosolizing DIM-C-pPhC$_6$H$_5$ for lung cancer treatment and to evaluate the anticancer effect of DIM-C-pPhC$_6$H$_5$ aerosol alone and in combination with i.v. docetaxel in an orthotopic murine lung tumor model. Our hypothesis is that inhalation delivery of DIM-C-pPhC$_6$H$_5$ will provide an enhanced antitumor effect along with i.v. administration of a traditional cytotoxic agent, such as docetaxel for the treatment of NSCLC. This combination therapy may significantly decrease the ther-

apeutic dose required for the cytotoxic agent (docetaxel) and thereby minimize adverse toxic side effects. The experimental design adapted to test this hypothesis includes evaluation of the antitumor effects of DIM-C-pPhC$_6$H$_5$ aerosol when administered alone or in combination with docetaxel in a murine lung tumor model. Our results show that DIM-C-pPhC$_6$H$_5$ alone or in combination with docetaxel was highly potent as anticancer agents, and the aerosol delivery method significantly increased the effectiveness of DIM-C-pPhC$_6$H$_5$.

Materials and Methods

Materials

DIM-C-pPhC$_6$H$_5$ was synthesized as previously described (24). Docetaxel was a gift from Aventis. The human NSCLC cell line A549 was obtained from the American Type Culture Collection, and all experiments with cell cultures were done within 6 months. The cell lines were characterized by the American Type Culture Collection using techniques such as short tandem repeat profiling, cell morphology evaluation, karyotyping, and cytochrome *c* oxidase I assay and also evaluated for contamination. A549 cells were grown in F12K medium (Sigma) supplemented with 10% fetal bovine serum. All tissue culture media contained antibiotic-antimycotic solution of penicillin (5,000 units/mL), streptomycin (0.1 mg/mL), and neomycin (0.2 mg/mL). The cells were maintained at 37°C in the presence of 5% CO$_2$. All other chemicals were either reagent or tissue culture grade.

Formulation of nebulizer solution

Aqueous formulations of DIM-C-pPhC$_6$H$_5$ suitable for nebulization were prepared by partly dissolving DIM-C-pPhC$_6$H$_5$ in 0.5 mL ethanol and 500 mg of α-tocopherol polyethylene glycol succinate (TPGS) and diluted up to 10 mL with distilled water to achieve an 0.05% (w/v) solution. This was used for *in vitro* characterization, and a 0.2% (w/v) solution was used for animal studies.

Characterization of aerodynamic properties using cascade impactor

Particle size distribution was measured using an eight-stage Anderson cascade impactor, Mark II, connected to the PARI LC STAR jet nebulizer mouthpiece. The impactor plates were coated with 10% Pluronic L10 in ethanol solution to prevent particle bounce. The aqueous formulation was nebulized using PARI LC STAR jet nebulizer at dry compressed air flow rate of 4 L/min for 5 minutes into the cascade impactor, which was operated at a flow rate of 28.3 L/min according to United States Pharmacopeia guidance. To determine the aerodynamic properties of DIM-C-pPhC$_6$H$_5$ formulation, the inhaled aerosol on the nebulizer, throat, jet stage, plates on impactor stages 0 to 7, and filter was collected by washing with 5 mL of mobile phase [acetonitrile/water (90:10)]. The analysis was done on a Waters high-performance liquid chromatography (HPLC) system using a Symmetry C18 column
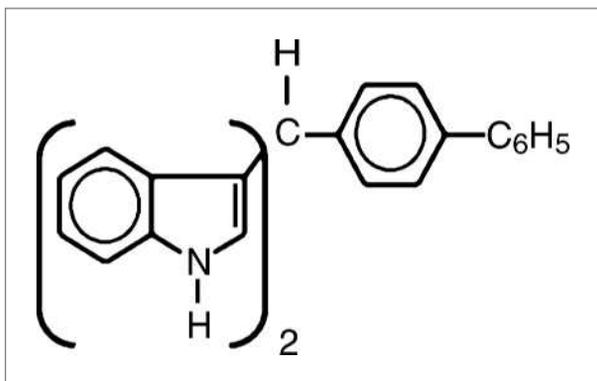

Figure 1. Chemical structures of DIM-C-pPhC$_6$H$_5$.

(5 μm, 4.6 × 250 mm) with a Nova-Pack C8 guard column at a wavelength of 240 nm and flow rate of 1 mL/min. The HPLC system consisted of a Waters autosampler (model 717 plus), Waters binary pump (model 1525), and Waters UV photodiode array detector (model 996). All samples will be analyzed in triplicate. The mass median aerodynamic diameter (MMAD) and geometric SD (GSD) were obtained from impactor data using established software in our lab. Impactor experiments were repeated at least two times.

In vivo orthotopic lung tumor model

The laboratory murine model has been used extensively in lung cancer research. Female, 6-week-old, athymic *nu/nu* mice were purchased from Harlan, Inc. The mice were housed and maintained in specific pathogen-free conditions in a facility approved by the American Association for Accreditation of Laboratory Animal Care. Food and water were provided *ad libitum* to the animals in standard cages. All experiments were done in accordance with the guidelines of the Institutional Animal Care and Use Committee of Florida A&M University.

Mice were anesthetized and a 5-mm skin incision was made to the left chest, ~5 mm below the scapula. Hamilton syringes (1 mL) with 28-gauge hypodermic needles were used to inject the cell inoculum through the sixth intercostal space into the left lung. The needle was quickly advanced to a depth of 3 mm and quickly removed after the injection of the A549 cells (1×10^6 per mouse) suspended in 100 μL PBS into the lung parenchyma. Only cell suspensions of >90% viability determined by trypan blue exclusion were used. Wounds from the incisions were closed with surgical skin clips (32, 33). Animals were observed for 45 to 60 minutes until fully recovered.

Administration and dosage of DIM-C-pPhC$_6$H$_5$ aerosol

DIM-C-pPhC$_6$H$_5$ formulation at a concentration of 2 mg/mL was used to generate aerosol by nebulization with a PARI LC STAR jet nebulizer using dry compressed air at a flow rate of 4 L/min. Female *nu/nu* mice (20 ± 2 g) were restrained in animal holders and placed in an inhalation chamber (SCIREQ) such that only the nose of each mouse was exposed to the aerosol cloud. The nebulizer was connected to the top part of the inhalation chamber from which the generated aerosol flowed down the central tower to the 12 mice peripherally arranged. The duration of aerosol exposure per treatment was 30 minutes.

The deposition fraction was measured by estimating the amount of DIM-C-pPhC$_6$H$_5$ deposited in lungs following nebulization by HPLC analysis. Briefly, DIM-C-pPhC$_6$H$_5$ formulation (2 mg/mL) was nebulized to female *nu/nu* mice (*n* = 12) placed in a inhalation chamber (SCIREQ) with a PARI LC STAR jet nebulizer using dry compressed air at a flow rate of 4 L/min for 30 minutes. After completion of the 30-minute exposure, animals were sacrificed with overdose of halothane. Lung tissues were collected and evaluated for DIM-C-pPhC$_6$H$_5$ content by an earlier

validated HPLC method using solvent extraction. Lungs were weighed and homogenized with 500 μL PBS (pH 7.4) and added to 50 μL of internal standard solution (100 μg/mL nimesulide) and vortexed. To the resultant samples, 1.5 mL of *tert*-butyl ether were added, vortexed, and then centrifuged (15 minutes at 3,500 rpm) to separate aqueous and organic phases. The organic layer was separated and evaporated to dryness, and the residue was then reconstituted with 200 μL of mobile phase and 100 μL were injected onto HPLC for quantification. HPLC system comprised an autosampler (model 717 plus), binary pump (model 1525), Waters UV photodiode array detector (model 996), and Symmetry C18 column (5 μm, 4.6 × 250 mm) at a flow rate of 1.0 mL/min, and the eluent was monitored at 242 nm. The gradient method was used with mobile phase consisting of acetonitrile, water (10:90%, v/v) at 0 minute, and (90:10%, v/v) at 8 minutes and remaining steady up to 17 minutes and changing back to (10:90%, v/v) at 20 minutes. Quantification of DIM-C-pPhC$_6$H$_5$ was accomplished by using a calibration standard curve between 0.05 and 8 μg/mL.

The deposition fraction was calculated using following equation:

$$\text{Deposition fraction (DF)} = A/C \times F \times T \qquad (1)$$

where *A* is the total amount of drug deposited in mice at the end of 30-minute nebulization (*A* = 2113.593 μg), *C* is the concentration of the drug in aerosol volume (for DIM-C-pPhC$_6$H$_5$ aerosol, *C* = 167 μg/L), *F* is the flow rate used for aerosolization (*F* = 4.5 L/min), and *T* is the duration of treatment (*T* = 30 minutes).

The estimated total deposited amount of inhaled drugs (*D*) for the ambient air was calculated by the following formula (7, 8):

$$D = C \times V \times \text{DF} \times T \qquad (2)$$

where *C* is the concentration of the drug in aerosol volume (for DIM-C-pPhC$_6$H$_5$ aerosol, *C* = 167 μg/L), *V* is the volume of air inspired by the animal during 1 minute (for mice, *V* = 1.0 L min/kg), DF is the measured deposition fraction using analytic method (DF = 0.093), and *T* is the duration of treatment (*T* = 30 minutes).

In this study, the deposition fraction and deposited dose of DIM-C-pPhC$_6$H$_5$ for duration of 30-minute nebulization treatment was ~0.093 and ~0.47 mg/kg, respectively.

Treatment of animals

Seven days after tumor implantation, the mice were randomly divided into the following groups (*n* = 12) to receive DIM-C-pPhC$_6$H$_5$ and docetaxel formulations. The control group received aerosolized vehicle (vitamin E TPGS solution); the second group received docetaxel (10 mg/kg i.v.) on days 14, 18, 22, and 29; the third group was exposed to DIM-C-pPhC$_6$H$_5$ aerosol three times a week; the fourth group received a combination of docetaxel i.v. and DIM-C-pPhC$_6$H$_5$ aerosol. To check for evidence of toxicity, the animals were weighed twice

weekly. On day 35, all animals were sacrificed by exposure to a lethal dose of halothane in a desiccator. After dissection and removal of the lungs, the lungs and tumor mass were washed in sterile PBS and weighed. The lung weights and tumor volume will be used for assessment of therapeutic activity of the treatments. We also evaluated efficacy of therapy in different areas by determining average number of tumor nodules in central, mid, and peripheral region of lungs harvested from control and treated groups. Tumor nodules of 2 to 10 mm^3 in volume were counted using harvested lungs for control and treated groups. For immunohistochemistry, terminal deoxynucleotidyl transferase (TdT)–mediated dUTP nick end labeling (TUNEL), and H&E staining procedures, some of the tumors were fixed in formalin, whereas others were rapidly frozen in liquid nitrogen and stored in –80°C.

TUNEL assay of orthotopic lung tumor tissues

Formalin-fixed tumor tissues harvested 35 days after tumor implantation were embedded in paraffin and sectioned. DeadEnd Colorimetric Apoptosis Detection System (Promega) was used to detect apoptosis in the tumor sections placed on slides according to the manufacturer's protocol. Briefly, the equilibration buffer was added to slides and incubated for 10 minutes followed by incubation for 10 minutes in 20 μg/mL proteinase K solution. The sections were washed in PBS and incubated with TdT enzyme at 37°C for 1 hour in a humidified chamber for incorporation of biotinylated nucleotides at the 3′-OH ends of DNA. The slides were incubated in horseradish peroxidase (HRP)–labeled streptavidin to bind the biotinylated nucleotides followed by detection with the stable chromagen 3,3′-diaminobenzidine. The images on the slides were visualized with an Olympus BX40 light microscope equipped with a computer-controlled digital camera (QImaging) and imaging software (Q capture). Three slides per group were stained, and apoptotic cells were identified by dark brown cytoplasmic staining.

Western blot analysis

Protein was extracted from tumor nodules collected from control untreated and treated tumors using radioimmunoprecipitation assay buffer [50 mmol/L Tris-HCl (pH 8.0), 150 mmol/L sodium chloride, 1.0% Igepal CA-630 (NP40), 0.5% sodium deoxycholate, 0.1% SDS] with protease inhibitor (500 mmol/L phenylmethylsulfonyl fluoride). The lysate from normal lung tissues was also prepared in a similar manner as described above. Protein content was measured using BCA Protein Assay Reagent kit (Pierce). Equal amounts of supernatant protein (50 μg) from the control and different treatments were denatured by boiling for 5 minutes in SDS sample buffer, separated by 10% SDS-PAGE, and transferred to nitrocellulose membranes for immunoblotting. Membranes were blocked with 5% skim milk in TBS with Tween 20 [10 mmol/L Tris-HCl (pH 7.6), 150 mmol/L Nacl, 0.5% Tween 20] and probed with antibodies against Akt (1:500), cyclin D1 (1:500), c-Jun NH$_2$-terminal kinase 2 (JNK2; 1:500),

Bad (1:500), Mcl-1 (1:500), survivin (1:500), NF-κB (1:500), IκBα (1:200), phospho-IκBα (P-IκBα; 1:200), vascular endothelial growth factor (VEGF; 1:500), and β-actin (1:1,000; Santa Cruz Biotechnology). HRP-conjugated secondary antibodies (Santa Cruz Biotechnology) were used. Proteins were visualized using enhanced chemiluminescent solution (Pierce) and exposed to Kodak X-OMAT AR autoradiography film (Eastman Kodak).

Immunohistochemistry for VEGF expression

Tissue sections (4–5 μm thick) mounted on poly-L-lysine–coated slide were deparaffinized by xylene, dehydrated through graded concentrations of alcohol, and incubated with 3% hydrogen peroxidase for 20 minutes to block endogenous peroxidase activity. Antigen retrieval for VEGF and cleaved caspase-3 staining was carried out for 10 minutes in 0.01 mol/L sodium citrate buffer (pH 6) heated at 95°C in a steam bath followed by cooling for 30 minutes. Endogenous peroxidase was blocked by 3% hydrogen peroxide in PBS for 10 minutes. The slides were washed with PBS and incubated for 1 hour at room temperature with a protein blocking solution. Excess blocking solution was drained, and the samples were incubated overnight at 4°C with either 1:50 dilution of VEGF antibody incubated with biotinylated secondary antibody followed by streptavidin. The color was developed by exposing the peroxidase to a substrate-chromagen, which forms a brown reaction product. The sections were then counterstained with hematoxylin. VEGF and cleaved caspase-3 expression was identified by the brown cytoplasmic staining.

Immunohistochemistry for CD31 expression and assessment of microvessel density

Tissue sections (4–5 μm thick) mounted on poly-L-lysine–coated slide were deparaffinized and blocked for peroxidase activity as described under methodology for immunohistochemistry for VEGF expression. After washing with PBS, the sections were pretreated in citrate buffer in a microwave oven for 20 minutes at 92°C to 98°C. After two washes with PBS, specimens were incubated in 10% normal goat serum (Atlanta Biologicals) for 20 minutes to reduce the nonspecific antibody binding. Subsequently, the sections were then incubated with a 1:500 diluted mouse CD31 monoclonal antibody (Cell Signaling Technology), which is recognized as an endothelial cell surface marker, at room temperature for 1 hour, followed by a 30-minute treatment with HRP rabbit/mouse (Santa Cruz Biotechnology). After three washes with PBS, the section was developed with diaminobenzidene–hydrogen peroxidase substrate and lightly counterstained with hematoxylin. To calculate microvessel density (MVD), three most vascularized areas of the tumor ("hotspots") were selected and mean values were obtained by counting vessels. A single microvessel was defined as a discrete cluster of cells positive for CD31 staining, with no requirement for the presence of a lumen. Microvessel counts were done at ×400 (×40 objective lens and ×10 ocular lens; 0.74 mm^2 per field).

Statistics

One-way ANOVA followed by Tukey's multiple comparison test was done to determine the significance of differences among groups using GraphPad Prism version 3.0 software. Differences were considered significant in all experiments at $P < 0.05$ (*, significantly different from untreated controls; **, significantly different from DIM-C-pPhC$_6$H$_5$ and docetaxel single treatments unless otherwise stated).

Results

Aerosol characteristics

An aqueous 0.2% (2 mg/mL) solution of DIM-C-pPhC$_6$H$_5$ with suitable characteristics for nebulization was developed. The aerodynamic properties included a MMAD of 1.78 ± 0.34 and GSD of 2.31 ± 0.02 (Fig. 2).

Docetaxel + DIM-C-pPhC$_6$H$_5$ aerosol inhibits growth of A549 orthotopic lung tumors

The anticancer activity of DIM-C-pPhC$_6$H$_5$ aerosol alone and in combination with docetaxel was investigated in female athymic nude mice bearing A549 orthotopic lung tumors. After 30 minutes of DIM-C-pPhC$_6$H$_5$ nebulization, the deposition fraction and deposited dose of DIM-C-pPhC$_6$H$_5$ were found to be ~0.093 and ~0.47 mg/kg, respectively. Initial pilot studies showed that nude mice implanted with 10^6 A549 cells develop fairly uniform tumors within 1 week. After 7 days of tumor inoculation, the average lung weight and tumor volume
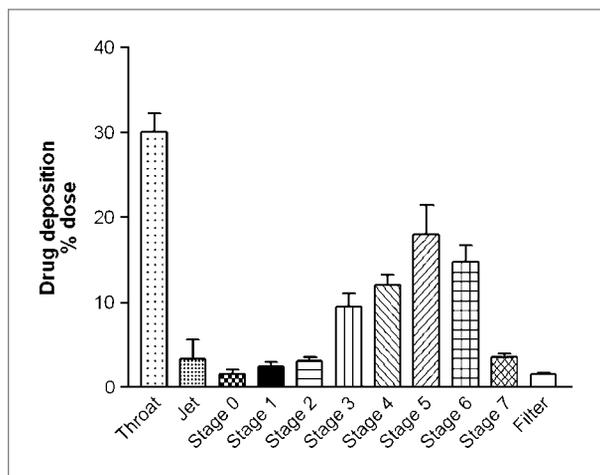

Figure 2. Aerodynamic properties of DIM-C-pPhC$_6$H$_5$ aerosol using Andersen cascade impactor. The aerodynamic particle size distribution of DIM-C-pPhC$_6$H$_5$ aerosol was measured using an eight-stage Anderson cascade impactor, Mark II, following nebulization for 5 min at a flow rate of 28.3 L/min using the PARI LC STAR jet nebulizer. The total drug deposited on various stages, actuator, and throat was determined using HPLC. Data were expressed as the percentage of the total drug deposited on all stages of the impactor, including actuator and throat. Columns, mean ($n = 3$); bars, SD. Calculated aerodynamic characteristics from impaction data: MMAD, 1.78 ± 0.34 μm; GSD, 2.31 ± 0.02.
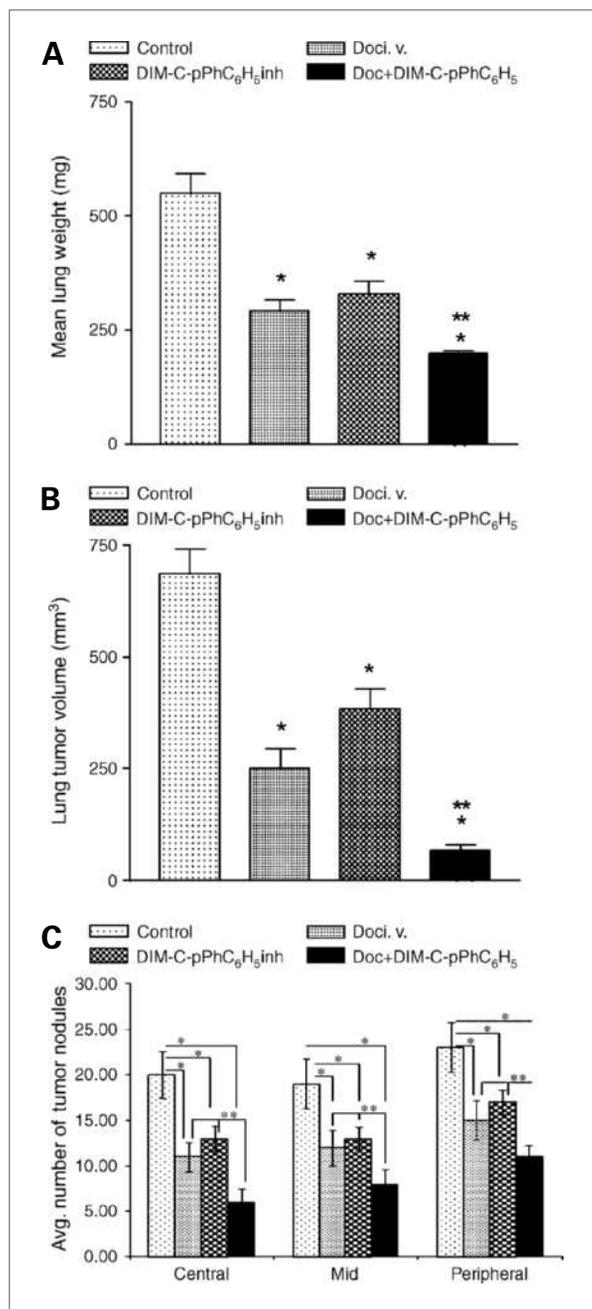

Figure 3. Effects of DIM-C-pPhC$_6$H$_5$ and docetaxel (Doc) on human orthotopic lung tumor weight (A), human orthotopic lung tumor volume (B), and tumor nodules in central, mid, and peripheral regions of lungs (C). A549 cells (1×10^6) were injected into the lungs of nude mice. Tumors were established for 7 d before therapy. Tumors from animals treated with 2 mg/mL C-DIM aerosol (three times a week), 10 mg/kg docetaxel (days 14, 18, 22, and 29), or combination were harvested after 35 d. Lung weights and tumor volumes were determined for measurement of therapeutic activity of the treatments. Tumor nodules of 2 to 10 mm^3 in volume were counted using harvested lungs for control and treated groups, and the average number of tumor nodules was determined. One-way ANOVA followed by Tukey post test was used for statistical analysis. $P < 0.05$ (*, significantly different from untreated controls; **, significantly different from DIM-C-pPhC$_6$H$_5$ and docetaxel single treatments). Columns, mean ($n = 12$); bars, SD.

Ichite et al.

were 245 ± 15.89 mg and 215 ± 21.48 mm^3, respectively. Treatment was started 7 days after tumor implantation and continued for a total of 28 days. The results (Fig. 3A) show that lung tumor weights were signifi-

cantly (*, $P < 0.001$) decreased after treatment with docetaxel, DIM-C-pPhC$_6$H$_5$ aerosol, and docetaxel + DIM-C-pPhC$_6$H$_5$ aerosol compared with control. Combination treatment was the most effective inhibitor of lung tumor
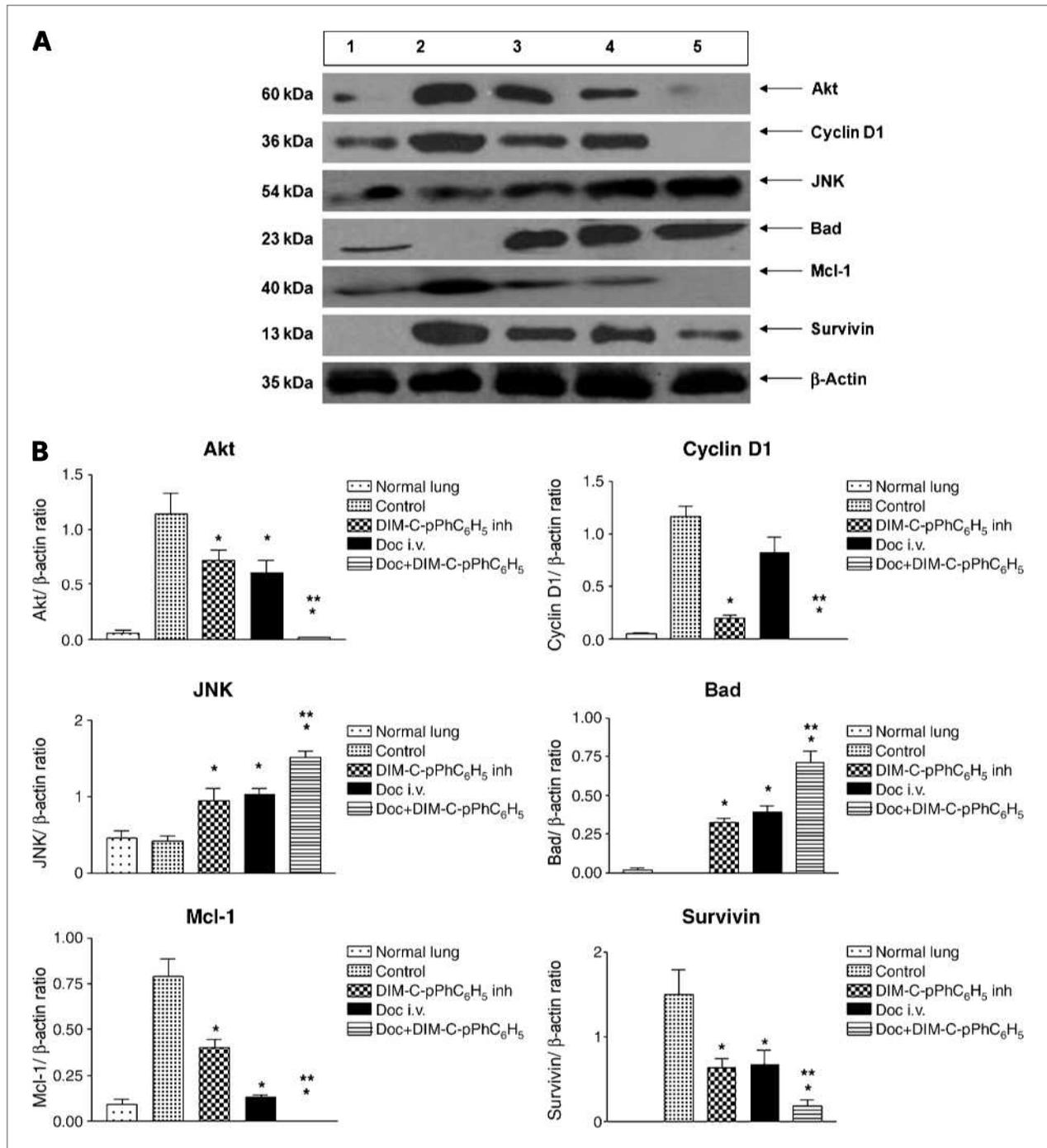

Figure 4. A, expression of apoptotic proteins (Akt, cyclin D1, JNK2, Bad, Mcl-1, and surviving) in tumor nodule and normal lung lysates by Western blotting. B, quantitation of apoptotic protein expression. Lane 1, normal lung tissue; lane 2, untreated control tumors; lane 3, DIM-C-pPhC$_6$H$_5$ aerosol; lane 4, docetaxel; lane 5, docetaxel + DIM-C-pPhC$_6$H$_5$. β-Actin protein acts as a loading control. Similar results were observed in replicate experiments. Protein expression levels (relative to β-actin) were determined. Columns, mean of three replicate determinations; bars, SE. One-way ANOVA followed by Tukey post test was used for statistical analysis. $P < 0.05$ (*, significantly different from untreated controls; **, significantly different from DIM-C-pPhC$_6$H$_5$ and docetaxel single treatments).
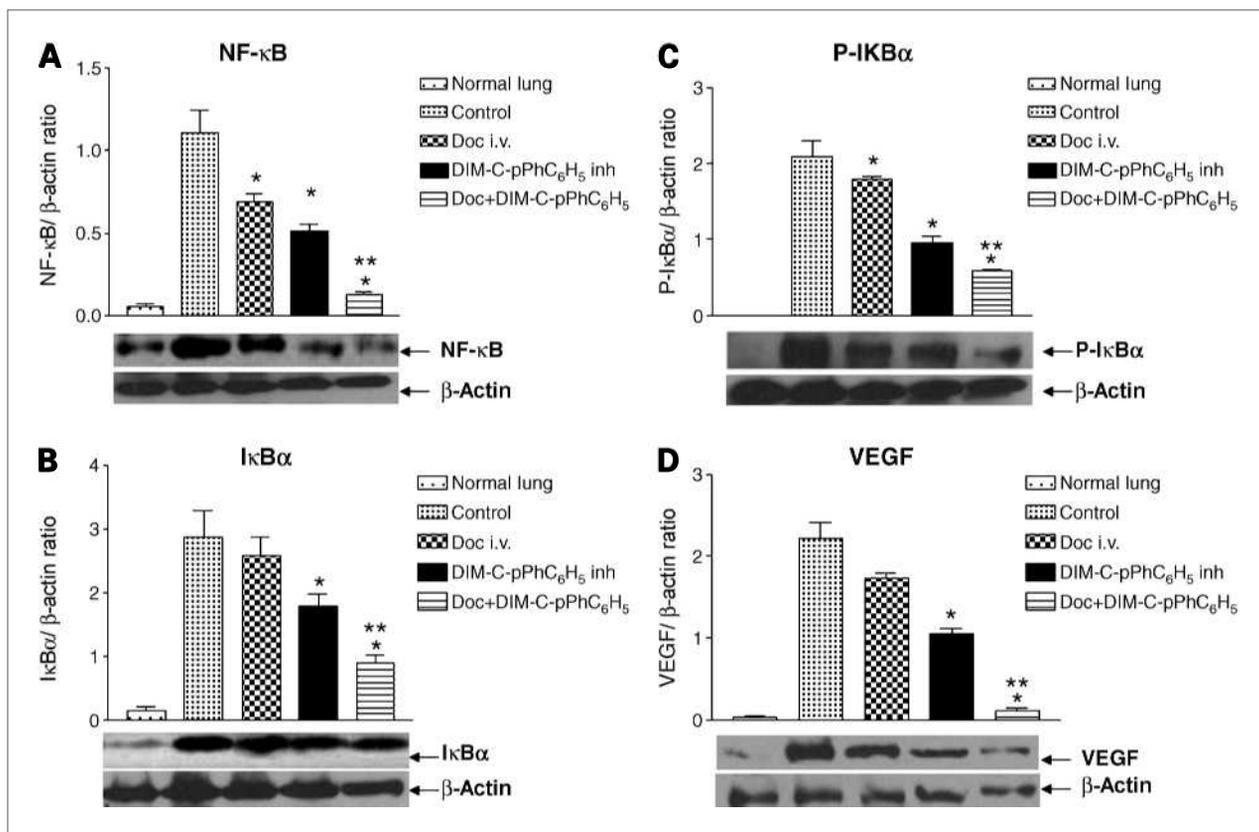
Figure 5. Expression of apoptotic and angiogenic proteins in tumors. Tumor nodule lysates from control untreated and treated tumors were analyzed by Western blotting for NF-κB (A), IκBα (B), P-IκBα (C), and VEGF (D) protein expression. Lane 1, normal lung tissue; lane 2, untreated control tumors; lane 3, DIM-C-pPhC$_6$H$_5$ aerosol ; lane 4, docetaxel; lane 5, docetaxel + DIM-C-pPhC$_6$H$_5$. β-Actin protein acts as a loading control. Quantitation of protein expression relative to β-actin was determined. Columns, mean (n = 3); bars, SE. One-way ANOVA followed by Tukey post test was used for statistical analysis. $P < 0.05$ (*, significantly different from untreated controls; **, significantly different from DIM-C-pPhC$_6$H$_5$ and docetaxel single treatments).

growth compared with docetaxel or DIM-C-pPhC$_6$H$_5$ aerosol treatments alone. Lung tumor weight reduction in mice treated with combination of docetaxel + DIM-C-pPhC$_6$H$_5$ was 64% compared with 40% and 47% in mice treated with DIM-C-pPhC$_6$H$_5$ aerosol and docetaxel alone, respectively. Lung tumor volume reduction (Fig. 3B) in mice treated with the combination of treatment was 90% compared with 44% and 63% in mice treated with DIM-C-pPhC$_6$H$_5$ aerosol and docetaxel alone, respectively. A nonsignificant ($P > 0.05$) change in average number of tumor nodules was observed among central, mid, and peripheral regions of harvested lungs from each treated groups (Fig. 3C). DIM-C-pPhC$_6$H$_5$ aerosol and docetaxel treatment showed a significant (*, $P < 0.001$) decrease in average number of tumor nodules in central, mid, and peripheral regions compared with single-agent treatment and control groups. We did not observe any weight loss or other signs of toxicity in mice treated with DIM-C-pPhC$_6$H$_5$ aerosol (data not shown). The average weight loss observed in the docetaxel alone treatment group was com-

parable with that of the combination group, consistent with the expected toxicity of docetaxel.

Effects of treatments on apoptotic and angiogenic proteins in A549 orthotopic lung tumors

We compared the expression of several apoptotic proteins and VEGF in normal lung tissue lysates and tumor lysates from control and treated mice by Western blot analysis using β-actin as a loading control (Figs. 4 and 5). DIM-C-pPhC$_6$H$_5$ aerosol and docetaxel treatment nonsignificantly ($P > 0.05$) decreased Akt expression to 0.65- and 0.6-fold in regressed tumor samples, respectively. Interestingly, expression of Akt was significantly (*, $P < 0.001$) decreased in the combination treatment group (Fig. 4A and B). In regressed tumors, the combination (*, $P < 0.001$), docetaxel (*, $P < 0.001$), and DIM-C-pPhC$_6$H$_5$ (*, $P < 0.001$) significantly decreased cyclin D1 expression to a nondetectable level, 0.58- and 0.10-fold, respectively, of controls (Fig. 4A and B). Docetaxel + DIM-C-pPhC$_6$H$_5$ increased JNK2 protein expression significantly (**, $P < 0.05$) to 4.6-fold compared with

2.8-fold with DIM-C-pPhC$_6$H$_5$ (*, $P < 0.01$) and 3.08-fold with docetaxel (*, $P < 0.01$) treatment of controls in regressed tumors (Fig. 4A and B). The combination, docetaxel, and DIM-C-pPhC$_6$H$_5$ increased Bad expression significantly (*, $P < 0.001$), and this protein was nondetectable in tumors from control mice (Fig. 4A and B). DIM-C-pPhC$_6$H$_5$ and docetaxel treatment significantly (*, $P < 0.05$) decreased Mcl-1 expression to 0.52- and 0.09-fold in regressed tumor samples, respectively, and the Mcl-1 protein expression was nondetectable in the combination treatment group (Fig. 4A and B). The expression of survivin protein was significantly decreased by 0.13-fold (*, $P < 0.01$), 0.43-fold (*, $P < 0.05$), and 0.44-fold (*, $P < 0.05$) with combination, docetaxel, and DIM-C-pPhC$_6$H$_5$ aerosol treatment compared with control group (Fig. 4A and B). Results in Fig. 4A and B showed that expression of Akt, cyclin D1, Mcl-1, and survivin proteins was significantly ($P < 0.001$) increased in tumor tissues from control group compared with normal lung tissue. The tumor tissues from the control group showed a significant ($P < 0.01$) decrease in expression of JNK and Bad compared with normal lung tissue (Fig. 4A and B). Results illustrated in Fig. 5 show that the combination significantly decreased expression of NF-κB (Fig. 5A) to 0.06-fold (*, $P < 0.001$), IκBα (Fig. 5B) to 0.32-fold (*, $P < 0.01$), P-IκBα (Fig. 5C) to 0.37-fold (*, $P < 0.001$), and VEGF (Fig. 5D) to 0.04-fold (*, $P < 0.001$) compared with control, whereas the effects of docetaxel or DIM-C-pPhC$_6$H$_5$ alone on decreasing these parameters were response dependent. Tumor tissues from control mice exhibited a significant ($P < 0.001$) decrease in expression of NF-κB, IκBα, P-IκBα, and VEGF compared with normal lung tissue (Fig. 5).

H&E staining and induction of DNA fragmentation in regressed A549 lung tumors

The A549 lung tumor histology was evaluated by H&E staining of lung tumor tissue. Occasional and isolated microvessels were seen in tumor treated with DIM-C-pPhC$_6$H$_5$ aerosol, docetaxel, and the combination, while control group showed well-formed capillaries surrounding nests of tumor cells (Fig. 6A). Histologic examination of the lungs and tracheobronchial epithelium showed no signs of inflammation or edema among all groups, which suggests safer profile of DIM-C-pPhC$_6$H$_5$ aerosol and combination therapy. To investigate the role of apoptosis on tumor growth inhibition, the tumor sections harvested at the end of the study were stained with TUNEL for detection of DNA fragmentation (Fig. 6B). Single-agent therapy with either docetaxel or DIM-C-pPhC$_6$H$_5$ aerosol induced DNA fragmentation (brown staining) that was further increased by combination therapy.

Inhibition of angiogenesis by docetaxel + DIM-C-pPhC$_6$H$_5$ aerosol in A549 orthotopic lung tumors

To examine if the docetaxel + DIM-C-pPhC$_6$H$_5$ aerosol combination inhibited lung tumor growth through inhibition of angiogenesis, we determined VEGF expression in orthotopic A549 tumor tissue sections by
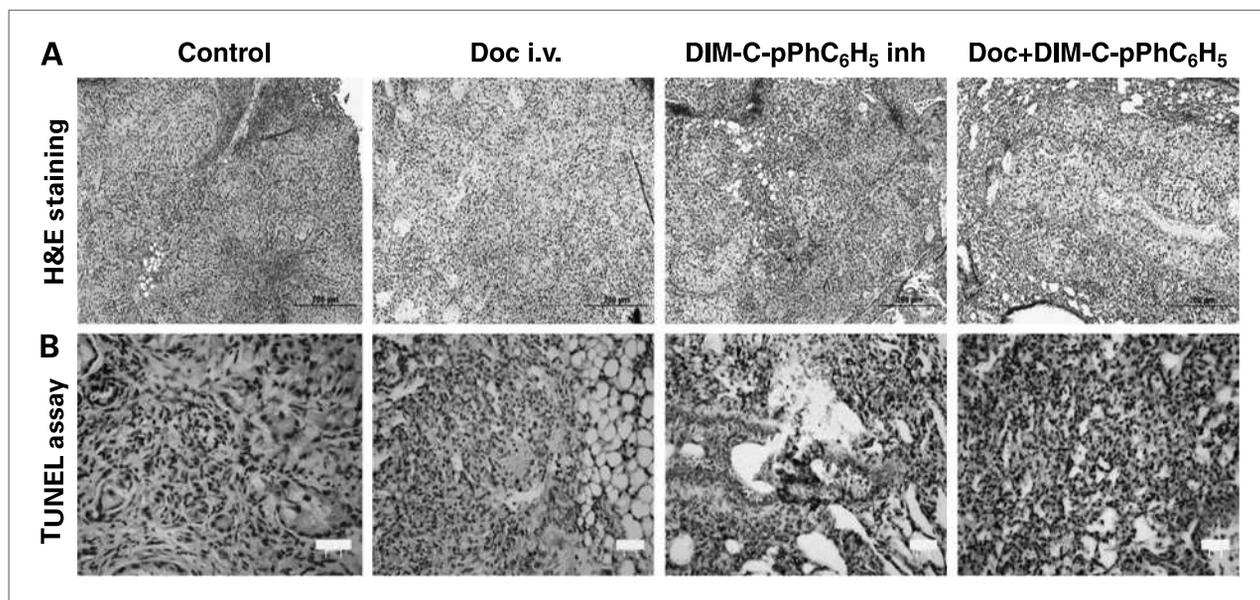

Figure 6. Analysis of lung tumor tissues. A, immunohistochemical H&E staining of orthotopic A549 lung tumor tissues. Occasional and isolated microvessels were seen in tumor treated with DIM-C-pPhC$_6$H$_5$ aerosol, docetaxel, and the combination, while control group showed well-formed capillaries surrounding nests of tumor cells. Original magnification, ×10. Scale bars, 200 μm. B, TUNEL staining of orthotopic A549 lung tumor tissues. Lungs were dissected from mice on day 35, fixed in 10% formalin, paraffin embedded, and sectioned. Sections were stained according to the protocol specified in DeadEnd Colorimetric Apoptosis Detection System. Control cells were untreated. Original magnification, ×40. Scale bars, 20 μm. Cells showing induction of apoptosis are stained.

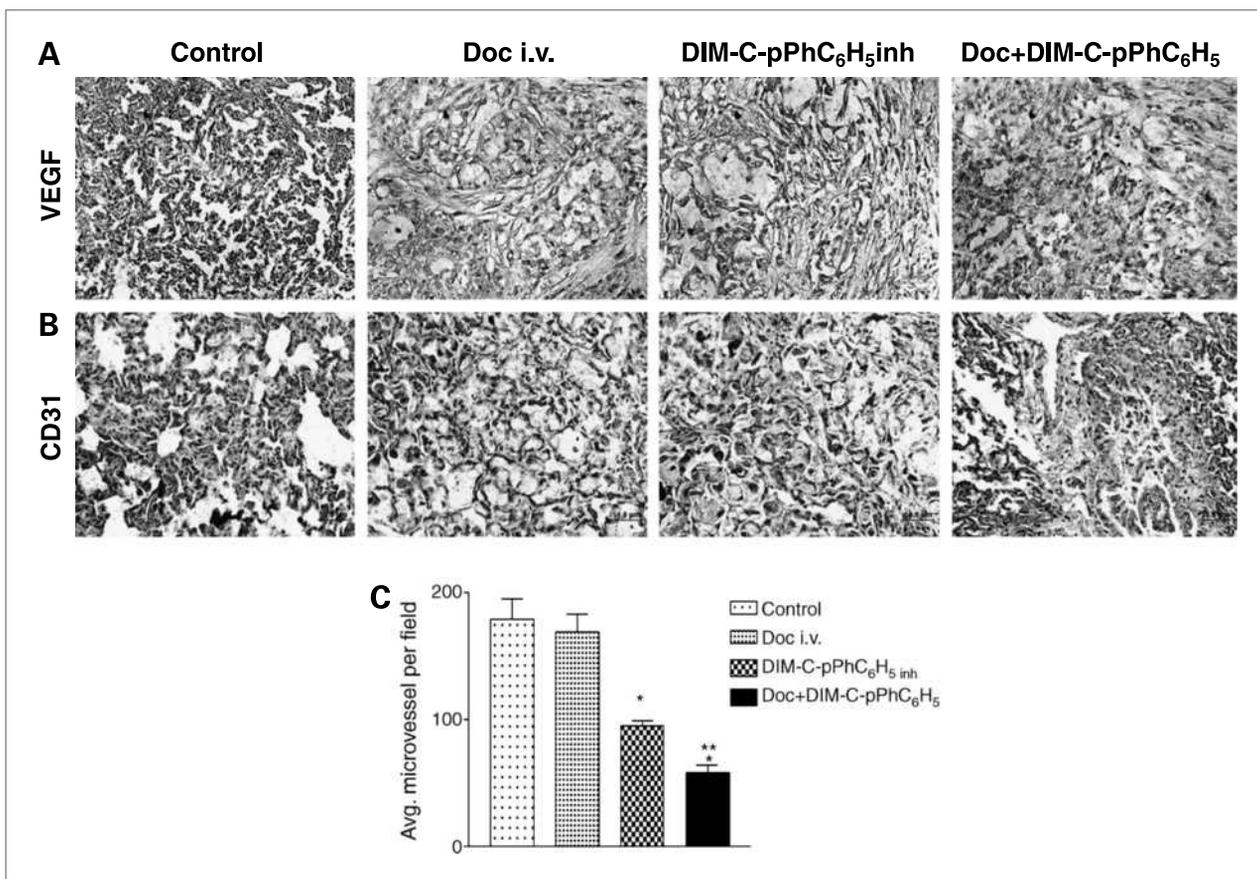**Figure 7.** Modulation of angiogenesis by DIM-C-pPhC$_6$H$_5$ aerosol, docetaxel, and their combination. A, immunohistochemical staining of orthotopic A549 lung tumor tissues for VEGF expression. Lungs were dissected from mice on day 35, fixed in 10% formalin, paraffin embedded, and sectioned. Sections were stained using the avidin-biotin complex staining kit as described in Materials and Methods. Cells showing positive VEGF expression are stained. Original magnification, ×40. Scale bars, 200 μm. B, immunohistochemical staining of orthotopic A549 lung tumor tissues for CD31 expression. Tumor angiogenesis was assessed by immunohistochemical staining with anti-CD31 antibody on paraffin-embedded sections. Occasional and isolated microvessels were seen in tumor treated with DIM-C-pPhC$_6$H$_5$ aerosol, docetaxel, and the combination, while control group showed well-formed capillaries surrounding nests of tumor cells. Original magnification, ×40. Scale bars, 200 μm. C, assessment of MVD in control, DIM-C-pPhC$_6$H$_5$ aerosol–, docetaxel-, and DIM-C-pPhC$_6$H$_5$ + docetaxel–treated mice. MVD was calculated by selecting three most vascularized areas of the tumor (hotspots), and mean values were obtained by counting vessels. A single microvessel was defined as a discrete cluster of cells positive for CD31 staining, with no requirement for the presence of a lumen. Microvessel counts were done at ×400 (×40 objective lens and ×10 ocular lens; 0.74 mm^2 per field). The MVD was significantly different between the control group and treated groups in sequential analysis. $P < 0.05$ (*, significantly different from untreated controls; **, significantly different from DIM-C-pPhC$_6$H$_5$ and docetaxel single treatments).

immunohistochemistry. The highest expression of VEGF was seen in tumor tissues harvested from untreated mice. Decreased expression of VEGF (Fig. 7A) was observed in tumors treated with the combination compared with tumors treated with docetaxel or DIM-C-pPhC$_6$H$_5$ alone. This response correlated with downregulation of VEGF protein observed in tumor lysates from mice treated with the same compounds (Fig. 5D).

MVD in tumor tissue

Using the immunohistochemical technique, CD31$^+$ endothelial cells were identified, as illustrated in Fig. 7B. The staining of microvessels in docetaxel + DIM-C-pPhC$_6$H$_5$ aerosol and DIM-C-pPhC$_6$H$_5$ aerosol groups was decreased compared with docetaxel treatment and control. The average number of microvessels per field in groups treated with docetaxel + DIM-C-pPhC$_6$H$_5$ aerosol, DIM-C-pPhC$_6$H$_5$ aerosol, and docetaxel was found to be 58 ± 10.5 (**, $P < 0.001$), 95 ± 6.6 (*, $P < 0.05$), and 169.3 ± 23.7, respectively, compared with 179.0 ± 28.4 in the control group (Fig. 7C).

Discussion

Despite increased interest in regional chemotherapy, relatively few studies have reported the feasibility of delivering drugs by inhalation for lung cancer treatment. Combinations of celecoxib (inhalation or oral) with i.v. docetaxel *in vivo* in an orthotopic NSCLC xenograft model resulted in a significant reduction ($P < 0.001$) in

lung weight and tumor volume in mice compared with celecoxib (oral or inhalation) or docetaxel treatment alone (33). Koshkina et al. (7) evaluated the effects of 9-nitrocamptothecin aerosol in B16 melanoma and osteosarcoma lung metastasis models. Reduced lung weights ($P = 0.005$) and number of tumor foci ($P < 0.001$) were observed in the B16 melanoma model. In the osteosarcoma model, the number of lung tumor foci ($P < 0.005$) and the size of individual tumor nodules ($P < 0.02$) were decreased. Administration of paclitaxel liposome aerosol resulted in lung weights similar to the normal lung weights (179 ± 16 and 153 ± 19 mg, respectively; $P > 0.05$) in a renal carcinoma lung metastasis model (8).

Previous *in vitro* studies with A549 and H460 lung cancer cells in our laboratory showed that the combination of DIM-C-pPhC$_6$H$_5$ + docetaxel synergistically or additively induced apoptosis and several proapoptotic proteins (32). Moreover, *in vivo* studies using docetaxel (i.v. bolus 10 mg/kg) and DIM-C-pPhC$_6$H$_5$ (40 mg/kg) three times weekly by oral gavage showed that both compounds alone and in the combination induced apoptosis and decreased lung weights (compared with vehicle control). In this study, we primarily focused in compound-induced *in vivo* changes in proapoptotic and kinase activities in an orthotopic murine lung tumor model using A549 cells as previously described (32). Aerosolization of poorly water-soluble drugs via nebulization and the consequent aerosol exposure to mice pose difficulties in proof-of-concept studies such as the current study. Dahl et al. (34) used ethanolic solutions of 13-*cis* retinoic acid for chemoprevention in A/J mice and thus resulted in a significant ($P < 0.005$) decrease in tumor multiplicity ranging from 56% to 80%. In the present study, attempts were made to prepare DIM-C-pPhC$_6$H$_5$ as an aqueous formulation using TPGS an ethoxylated derivative of vitamin E, which is suitable for inhalation delivery with a nebulizer. Characterization of the DIM-C-pPhC$_6$H$_5$ aerosol using Anderson cascade impactor showed MMAD of 1.78 ± 0.34 μm and GSD of 2.31 ± 0.02, respectively (Fig. 2). The DIM-C-pPhC$_6$H$_5$ aerosol formulation used in this study was found to be chemically stable for 1 month at room temperature (data not shown).

Several orthotopic mouse models have been developed for drug screening, and this model provides tumor cells with an optimal environment for growth and progression and may reflect the clinical situation (32). Hence, we have used this orthotopic murine lung tumor model with A549 cells to study the efficacy of aerosolized DIM-C-pPhC$_6$H$_5$ alone and in combination with docetaxel. In this study, a nose-only inhalation chamber was used for aerosol exposure because the procedure and system is simple and does not require anesthetization, and a large number of animals can be simultaneously exposed to the aerosol (33). The aerosolized DIM-C-pPhC$_6$H$_5$ formulation at ambient air following 30-minute nebulization showed deposition fraction of ~0.093, which was 3.2-fold lower than deposition fraction (0.3) reported with nebulization of anticancer drugs using 5% CO_2 (7, 8). DIM-C-pPhC$_6$H$_5$

was administered (alone and in combination with docetaxel) as an aerosol (deposited dose of ~0.47 mg/kg) three times per week, and this dosing regimen allowed us to directly compare the effectiveness of DIM-C-pPhC$_6$H$_5$ administered by oral gavage (32) or by an aerosol. Results summarized in Fig. 3 show that docetaxel and DIM-C-pPhC$_6$H$_5$ alone decreased mean lung tumor weights and volumes, and the combined treatment was more effective than the single-agent treatment. The efficacy of this therapy was determined from the average number of tumor nodules in central, mid, and peripheral region of lungs harvested from control and treated groups. DIM-C-pPhC$_6$H$_5$ aerosol alone and in combination with docetaxel showed nonsignificant ($P > 0.05$) change in average number of tumor nodules among the three (central, mid, and peripheral) regions (Fig. 3C), showing efficient pulmonary delivery of the DIM-C-pPhC$_6$H$_5$ aerosol even into the deep lungs. Moreover, DIM-C-pPhC$_6$H$_5$ aerosol + docetaxel treatment also exhibited a significant ($P < 0.01$) decrease in the average number of tumor nodules in all regions of the harvested lungs compared with single-agent treated and control groups. The overall pattern of antitumorigenic activity summarized in Fig. 3 using ~0.47 mg/kg of aerosol treatment with DIM-C-pPhC$_6$H$_5$ was similar to that of previously observed using 40 mg/kg DIM-C-pPhC$_6$H$_5$ administered by oral gavage (32). Thus, treatment with DIM-C-pPhC$_6$H$_5$ as an aerosol was significantly effective ($P < 0.001$) than administering the compound by oral gavage (32), and this dramatically illustrates the efficacy of the inhalation route of drug delivery.

Previous studies with DIM-C-pPhC$_6$H$_5$ and related C-substituted DIMs showed that these compounds induce multiple proapoptotic responses that activate the intrinsic and extrinsic pathways (20–22, 25, 35–37). In addition, other proteins such as cyclin D1 and the estrogen receptor are downregulated by C-substituted DIM through activation of the proteasome pathway (21, 24, 25), and C-substituted DIMs also enhance or modulate phosphorylation of several kinases including JNK. Result of our *in vivo* studies show that docetaxel and DIM-C-pPhC$_6$H$_5$ aerosol alone and the combination treatment induce proapoptotic (Bad) or decrease survival (survivin, Akt, and Mcl-1) proteins, and this was also accompanied by downregulation of cyclin D1 (Fig. 4A and B). DIM-C-pPhC$_6$H$_5$ also induced JNK2 phosphorylation in tumors (Fig. 4A and B), and this response has previously been observed for C-DIMs in pancreatic and colon cancer cells, where JNK phosphorylation plays a role in activation of the extrinsic proapoptotic pathway through induction of death receptor 5 (35, 36). In addition, we also observed that docetaxel, DIM-C-pPhC$_6$H$_5$, and their combination decreased two additional survival pathways in the lung tumors. Akt phosphorylation was decreased (Fig. 4A and B), and decreased expression of NF-κB (Fig. 5A), IκBα (Fig. 5B), and p-IκBα (Fig. 5C) proteins was also observed.

We also investigated the effects of docetaxel, DIM-C-pPhC$_6$H$_5$, and their combination on apoptosis in A549 lung tumors tissues determining DNA fragmentation using the TUNEL assay. DNA fragmentation was highly

induced by the drug combination compared with docetaxel or DIM-C-pPhC$_6$H$_5$ alone, thus confirming that apoptosis is an important pathway associated with the anticancer activity of these compounds (Fig. 6). We also observed that treatment with docetaxel or oral DIM-C-pPhC$_6$H$_5$ combination increased the number of apoptotic cells compared with docetaxel or DIM-C-pPhC$_6$H$_5$ alone, and this was consistent with results of a previous study using oral administration of DIM-C-pPhC$_6$H$_5$ (32).

In this study, we also evaluated the effects of docetaxel, DIM-C-pPhC$_6$H$_5$, and combination treatment on VEGF expression, which is important in the formation of new blood vessels from existing vascular network and is required for providing nutrients and oxygen to rapidly proliferating cells before a tumor is established (38). VEGF and angiogenesis are critical for establishing growth and metastasis of solid tumors. We observed that the combination treatment reduces expression of VEGF (Fig. 5D) in regressed tumors and thereby inhibits angiogenesis. Other researchers have observed *in vitro* and *in vivo* antiangiogenic activities of DIM (39) and docetaxel (40) in MCF-7 breast and HT1080 fibrosarcoma cancers, respectively. VEGF expression in tumor tissues obtained from control and treated mice was also determined by immunohistochemistry. Decreased expression of VEGF was observed in lung tumors from mice treated with docetaxel + DIM-C-pPhC$_6$H$_5$ aerosol compared with those treated with docetaxel, DIM-C-pPhC$_6$H$_5$ aerosol, or control (Fig. 7A), suggesting that induced tumor regression after treatment with docetaxel + DIM-C-pPhC$_6$H$_5$ aerosol may also be due, in part, to decreased expression of VEGF (Fig. 5D). MVD is a commonly used index of tumor angiogenic activity, and the density of neovessels can be counted in histologic sections of the tumor and quantified (41). The tumor CD31 expression (Fig. 7B) and the average microvessels per field (Fig. 7C) in docetaxel + DIM-C-pPhC$_6$H$_5$ aerosol–treated group were weak and significantly ($P < 0.001$) decreased compared with the control group, and this correlates with VEGF expression (Western blotting and immunohistochemistry) in the treated and control groups.

Thus, DIM-C-pPhC$_6$H$_5$ alone and in combination with docetaxel exhibited antiangiogenic activity, and the mechanism of VEGF downregulation is currently being investigated in our laboratories.

In summary, results of this study show that DIM-C-pPhC$_6$H$_5$ aerosol alone and in combination with docetaxel is highly effective for inhibiting lung tumor growth in a murine orthotopic model for lung cancer. The antitumor activities of these agents are associated with activation of growth-inhibitory, proapoptotic, and antiangiogenic pathways in lung tumors. Moreover, using the inhalation route of exposure, we have shown that DIM-C-pPhC$_6$H$_5$ at a deposited dose of ~0.47 mg/kg (inhalation) was equipotent to an oral dose of 40 mg/kg (32). Thus, the use of DIM-C-pPhC$_6$H$_5$ alone and in combination with chemotherapeutic agents could be a novel approach for treatment and possibly prevention of lung cancer in high-risk patients. Currently, we are carrying out additional preclinical studies to establish the benefits of administering DIM-C-pPhC$_6$H$_5$ and related compounds by the inhalation route.

Disclosure of Potential Conflicts of Interest

Acknowledgments

Grant Support

References

1. Whitehead CM, Earle KA, Fetter J, et al. Exisulind-induced apoptosis in a non-small cell lung cancer orthotopic lung tumor model augments docetaxel treatment and contributes to increased survival. Mol Cancer Ther 2003;2:479–88.

2. Sharma S, White D, Imondi AR, Placke ME, Vail DM, Kris MG. Development of inhalational agents for oncologic use. J Clin Oncol 2001;19:1839–47.

3. Labiris NR, Dolovich MB. Pulmonary drug delivery. Part I: physiological factors affecting therapeutic effectiveness of aerosolized medications. Br J Clin Pharmacol 2003;56:588–99.

4. Yang X, Ma JK, Malanga CJ, Rojanasakul Y. Characterization of proteolytic activities of pulmonary alveolar epithelium. Int J Pharm 2000;195:93–101.

5. Wang Z, Chen HT, Roa W, Finlay W. Farnesol for aerosol inhalation: nebulization and activity against human lung cancer cells. J Pharm Pharm Sci 2003;6:95–100.

6. Gagnadoux F, Leblond V, Vecellio L, et al. Gemcitabine aerosol: *in vitro* antitumor activity and deposition imaging for preclinical safety assessment in baboons. Cancer Chemother Pharmacol 2006;58:237–44.

7. Koshkina NV, Kleinerman ES, Waidrep C, et al. 9-Nitrocamptothecin liposome aerosol treatment of melanoma and osteosarcoma lung metastases in mice. Clin Cancer Res 2000;6:2876–80.

8. Koshkina NV, Waldrep JC, Roberts LE, Golunski E, Melton S, Knight V. Paclitaxel liposome aerosol treatment induces inhibition of pulmonary metastases in murine renal carcinoma model. Clin Cancer Res 2001;7:3258–62.

9. Knight V, Koshkina NV, Golunski E, Roberts LE, Gilbert BE. Cyclosporin A aerosol improves the anticancer effect of paclitaxel aerosol in mice. Trans Am Clin Climatol Assoc 2004;115:395–404.

10. Koshkina NV, Kleinerman ES. Aerosol gemcitabine inhibits the growth of primary osteosarcoma and osteosarcoma lung metastases. Int J Cancer 2005;116:458–63.

11. Tatsumura T, Koyama S, Tsujimoto M, Kitagawa M, Kagamimori S. Further study of nebulisation chemotherapy, a new chemotherapeutic

method in the treatment of lung carcinomas: fundamental and clinical. Br J Cancer 1993;68:1146–9.

12. Verschraegen CF, Gilbert BE, Loyer E, et al. Clinical evaluation of the delivery and safety of aerosolized liposomal 9-nitro-20(*S*)-camptothecin in patients with advanced pulmonary malignancies. Clin Cancer Res 2004;10:2319–26.

13. Otterson GA, Villalona-Calero MA, Sharma S, et al. Phase I study of inhaled doxorubicin for patients with metastatic tumors to the lungs. Clin Cancer Res 2007;13:1246–52.

14. Wittgen BP, Kunst PW, van der Born K, et al. Phase I study of aerosolized SLIT cisplatin in the treatment of patients with carcinoma of the lung. Clin Cancer Res 2007;13:2414–21.

15. Allred CD, Kilgore MW. Selective activation of PPARγ in breast, colon, and lung cancer cell lines. Mol Cell Endocrinol 2005;235:21–9.

16. Hatton JL, Yee LD. Clinical use of PPARγ ligands in cancer. PPAR Res 2008;2008:159415.

17. Keshamouni VG, Arenberg DA, Reddy RC, Newstead MJ, Anthwal S, Standiford TJ. PPAR-γ activation inhibits angiogenesis by blocking ELR+CXC chemokine production in non-small cell lung cancer. Neoplasia 2005;7:294–301.

18. McGuire KP, Ngoubilly N, Neavyn M, Lanza-Jacoby S. 3,3′-Diindolylmethane and paclitaxel act synergistically to promote apoptosis in HER2/Neu human breast cancer cells. J Surg Res 2006; 132:208–13.

19. Copland JA, Marlow LA, Kurakata S, et al. Novel high-affinity PPARγ agonist alone and in combination with paclitaxel inhibits human anaplastic thyroid carcinoma tumor growth via p21WAF1/CIP1. Oncogene 2006;25:2304–17.

20. Chintharlapalli S, Papineni S, Safe S. 1,1-Bis(3′-indolyl)-1-(*p*-substituted phenyl)methanes inhibit colon cancer cell and tumor growth through PPARγ-dependent and PPARγ-independent pathways. Mol Cancer Ther 2006;5:1362–70.

21. Chintharlapalli S, Smith R III, Samudio I, Zhang W, Safe S. 1,1-Bis (3′-indolyl)-1-(*p*-substituted phenyl)methanes induce peroxisome proliferator-activated receptor γ-mediated growth inhibition, transactivation, and differentiation markers in colon cancer cells. Cancer Res 2004;64:5994–6001.

22. Kassouf W, Chintharlapalli S, Abdelrahim M, Nelkin G, Safe S, Kamat AM. Inhibition of bladder tumor growth by 1,1-bis(3′-indolyl)-1-(*p*-substituted phenyl)methanes: a new class of peroxisome proliferator-activated receptor γ agonists. Cancer Res 2006;66:412–8.

23. Chintharlapalli S, Papineni S, Safe S. 1,1-Bis(3′-indolyl)-1-(*p*-substituted phenyl)methanes inhibit growth, induce apoptosis, and decrease the androgen receptor in LNCaP prostate cancer cells through peroxisome proliferator-activated receptor γ-independent pathways. Mol Pharmacol 2007;71:558–69.

24. Qin C, Morrow D, Stewart J, et al. A new class of peroxisome proliferator-activated receptor γ (PPARγ) agonists that inhibit growth of breast cancer cells: 1,1-bis(3′-indolyl)-1-(*p*-substituted phenyl) methanes. Mol Cancer Ther 2004;3:247–60.

25. Vanderlaag K, Su Y, Frankel AE, et al. 1,1-Bis(3′-indolyl)-1-(*p*-substituted phenyl)methanes inhibit proliferation of estrogen receptor-negative breast cancer cells by activation of multiple pathways. Breast Cancer Res Treat 2008;109:273–83.

26. Hida T, Kozaki K, Ito H, et al. Significant growth inhibition of human lung cancer cells both *in vitro* and *in vivo* by the combined use of a selective cyclooxygenase 2 inhibitor, JTE-522, and conventional anticancer agents. Clin Cancer Res 2002;8:2443–7.

27. Hida T, Kozaki K, Muramatsu H, et al. Cyclooxygenase-2 inhibitor induces apoptosis and enhances cytotoxicity of various anticancer agents in non-small cell lung cancer cell lines. Clin Cancer Res 2000;6:2006–11.

28. Nawrocki ST, Sweeney-Gotsch B, Takamori R, McConkey DJ. The proteasome inhibitor bortezomib enhances the activity of docetaxel in orthotopic human pancreatic tumor xenografts. Mol Cancer Ther 2004;3:59–70.

29. Shaik MS, Chatterjee A, Jackson T, Singh M. Enhancement of antitumor activity of docetaxel by celecoxib in lung tumors. Int J Cancer 2006;118:396–404.

30. Sweeney CJ, Mehrotra S, Sadaria MR, et al. The sesquiterpene lactone parthenolide in combination with docetaxel reduces metastasis and improves survival in a xenograft model of breast cancer. Mol Cancer Ther 2005;4:1004–12.

31. Hotchkiss KA, Ashton AW, Mahmood R, Russell RG, Sparano JA, Schwartz EL. Inhibition of endothelial cell function *in vitro* and angiogenesis *in vivo* by docetaxel (Taxotere): association with impaired repositioning of the microtubule organizing center. Mol Cancer Ther 2002;1:1191–200.

32. Ichite N, Chougule MB, Jackson T, Fulzele SV, Safe S, Singh M. Enhancement of docetaxel anticancer activity by a novel diindolylmethane compound in human non-small cell lung cancer. Clin Cancer Res 2009;15:543–52.

33. Fulzele SV, Chatterjee A, Shaik MS, Jackson T, Singh M. Inhalation delivery and anti-tumor activity of celecoxib in human orthotopic non-small cell lung cancer xenograft model. Pharm Res 2006;23: 2094–106.

34. Dahl AR, Grossi IM, Houchens DP, et al. Inhaled isotretinoin (13-*cis* retinoic acid) is an effective lung cancer chemopreventive agent in A/J mice at low doses: a pilot study. Clin Cancer Res 2000;6: 3015–24.

35. Lei P, Abdelrahim M, Cho SD, Liu S, Chintharlapalli S, Safe S. 1,1-Bis (3′-indolyl)-1-(*p*-substituted phenyl)methanes inhibit colon cancer cell and tumor growth through activation of c-jun N-terminal kinase. Carcinogenesis 2008;29:1139–47.

36. Abdelrahim M, Newman K, Vanderlaag K, Samudio I, Safe S. 3,3′-Diindolylmethane (DIM) and derivatives induce apoptosis in pancreatic cancer cells through endoplasmic reticulum stress-dependent upregulation of DR5. Carcinogenesis 2006;27:717–28.

37. Lei P, Abdelrahim M, Safe S. 1,1-Bis(3′-indolyl)-1-(*p*-substituted phenyl)methanes inhibit ovarian cancer cell growth through peroxisome proliferator-activated receptor-dependent and independent pathways. Mol Cancer Ther 2006;5:2324–36.

38. Folkman J. Angiogenesis in cancer, vascular, rheumatoid and other disease. Nat Med 1995;1:27–31.

39. Chang X, Tou JC, Hong C, et al. 3,3′-Diindolylmethane inhibits angiogenesis and the growth of transplantable human breast carcinoma in athymic mice. Carcinogenesis 2005;26:771–8.

40. Grant DS, Williams TL, Zahaczewsky M, Dicker AP. Comparison of antiangiogenic activities using paclitaxel (taxol) and docetaxel (taxotere). Int J Cancer 2003;104:121–9.

41. Sezer O, Jakob C, Niemöller K. Angiogenesis in cancer. J Clin Oncol 2001;19:3299–301.

Molecular Cancer Therapeutics

Inhalation Delivery of a Novel Diindolylmethane Derivative for the Treatment of Lung Cancer

Nkechi Ichite, Mahavir Chougule, Apurva R. Patel, et al.

Updated version	Access the most recent version of this article at: doi:10.1158/1535-7163.MCT-09-1104

Cited articles	This article cites 41 articles, 21 of which you can access for free at: http://mct.aacrjournals.org/content/9/11/3003.full#ref-list-1

E-mail alerts	Sign up to receive free email-alerts related to this article or journal.
Reprints and Subscriptions	To order reprints of this article or to subscribe to the journal, contact the AACR Publications Department at pubs@aacr.org.
Permissions	To request permission to re-use all or part of this article, use this link http://mct.aacrjournals.org/content/9/11/3003. Click on "Request Permissions" which will take you to the Copyright Clearance Center's (CCC) Rightslink site.